

Fluorescence Studies and Electronic Absorption Spectroscopic Investigation of the Interaction between the Schiff base Nano-Complex of Zn (II) with FS-DNA

Neda Barakzaie, Niloufar Akbarzadeh-T*

Department of Chemistry, University of Sistan and Baluchestan, P.O. Box 98135-674, Zahedan, Iran

Received: 30 July 2024

Accepted: 22 August 2024

DOI: [10.30473/IJAC.2025.73057.1313](https://doi.org/10.30473/IJAC.2025.73057.1313)

Abstract

In this project, in the first part, the Schiff base ligand (3-nitrobenzaldehyde + 2-aminothiophenol = H₂L) was prepared. Then a nano-complex with the formula [Zn(HL)₂Cl₂] was synthesized using sonochemical method. Zn-nano-complex was identified by FT-IR, UV-Vis, 1H-NMR and Emission Scanning Electron Microscope (SEM). The spectroscopic results showed that the H₂L ligand was coordinated to the metal through the N atom. The FT-IR spectrum of Zn-nano-complex showed the vibrational band of the imminity group (C = N) at 1680-1600 cm⁻¹. The studies obtained from the UV-Vis spectrum confirm n → π* and π → π* intra-ligand transitions. FS-DNA (salmon sperm DNA) and Zn-nano-complex were examined using UV-Vis spectroscopy, fluorescence spectroscopy, and gel electrophoresis. The Stern–Volmer equation was used to calculate the binding constant (K_b) and apparent bimolecular quenching constant (k_q) for FS-DNA. Van der Waals forces and hydrogen bonds are important in the interaction between the DNA and the Zn (II) complex, according to an analysis of thermodynamic parameters (ΔH°, ΔS° and ΔG°). The interaction mechanism was determined to be the groove-binding mode. These results highlight the complex's complicated effects on DNA structure and the need to use a variety of analytical techniques in order to fully investigate metal-DNA interactions.

Keywords

Schiff Base; FS-DNA; Van Der Waals Interactions; Gel Electrophoresis.

1. INTRODUCTION

Certain aldehydes or ketones directly condense with the main amines to form Schiff base ligands with an azomethine group [1-2]. In several areas of chemistry, schiff base ligands and their metal complexes are unquestionably important. These compounds frequently function as ligands in coordination chemistry [3-4]. Schiff base ligands containing nitrogen and other donor atoms can bind to metal ions and form stable metal complexes [5-7]. Schiff base ligands play a significant role in various biological activities [8-9]. The biological activity of metal ions is also of importance, in addition to the biological impacts of the Schiff base ligand [10]. Complex formation with transition metal ions including copper, nickel, and zinc frequently increases the biological activity of Schiff base ligands [11]. The biological activity of complexes comprising oxygen and nitrogen donor Schiff base ligands generated from 2-hydroxy-1-naphthaldehyde was successfully investigated [12-13]. Because of their potential uses in bioinorganic chemistry, transition metal complexes binding to DNA has been thoroughly investigated [14-16]. Metal complexes can harm DNA in cancer cells, halt cell division, and ultimately cause cell death.

Since the efficiency of anticancer factors depends on the binding mechanism, DNA-binding studies are essential for discovering these factors [17]. DNA interacts via a variety of locations with metal complexes and anticancer medications. It is easy to examine changes in DNA structure using a variety of experimental techniques. The three non-covalent forms of binding that small molecules and metal complexes usually use to bind to DNA are (i) intercalative binding, (ii) groove binding, and (iii) electrostatic binding [18-19].

DNA is a macromolecule that contains the genetic instructions used in the development and function of all known living organisms and encodes many viruses. This molecule not only controls the construction of other molecules (proteins), but also plays a role in their own formation and repair. If a small change occurs in its structure, it can have serious consequences for the health and survival of the organism. And if it is damaged beyond repair, the diseased cell will die. Metal complexes can damage DNA, prevent cancer cells from proliferating, and eventually result in cell death. The binding mechanism identified by DNA-binding research is crucial for the development of

* Corresponding author:

more potent anticancer agents. In this work, we used sonochemical method to prepare $[Zn(HL)_2Cl_2]$ (a). The investigation also looked at Zn-nano-complex's interactions with FS- DNA. The characteristics of DNA binding were investigated using gel electrophoresis, UV-Vis, and fluorescence methods. The groove binding mode was indicated by the viscosity and CD data.

2. EXPERIMENTAL

2.1. Materials and methods

All of the chemicals purchased for the experiment were of the reagent grade and didn't require any additional purification. Zinc (II) chloride, 2-aminothiophenol, and 3-nitrobenzaldehyde were purchased from Sigma Aldrich, whereas solvents were purchased from Merck. Sigma Chemical Co. provided the DNA from salmon fish sperm. The material was human lung epithelial carcinoma. KBr discs containing produced compounds were utilized to perform FT-IR spectrum ($4000-400\text{ cm}^{-1}$) using a Perkin-Elmer FT-IR spectrophotometer, model spectrum two. At room temperature (298 K), the Optizen-view 2120 UV plus spectrometer scanned absorption spectra (UV-Vis) utilizing quartz cells with a 1 cm path length in the 200–800 nm range. We used an Ubbelohde viscometer to measure the viscosity. With a wavelength range of 210-380 nm, a JASCO-J815 spectrometer was used to obtain the CD measurements at room temperature. An LS-45 spectrophotometer made by PerkinElmer was used to measure the fluorescence spectra.

1.2 Synthesis of Schiff base ligand (H_2L)

For synthesis of the Schiff base ligand a solution of 3-nitrobenzaldehyde (0.075 g, 0.500 mmol) in 10 mL of ethanol was added to a solution of 2-aminothiophenol (0.053 mL, 0.500 mmol) in ethanol solution. Resulting mixture was refluxed for about 6 h. After five days to generate yellow crystals of H_2L .

1.3 Synthesis of complex $[Zn(HL)_2Cl_2]NPs$

Zinc (II) chloride ($ZnCl_2$) (0.020 g, 0.150 mmol) in 10 mL of methanol was run for 10 minutes in a high-density ultrasonic probe set to 100 W of power. 10 ml of a methanolic Schiff base ligand [H_2L] solution (0.077 g, 0.3 mmol) was added dropwise to this irradiation solution. The resulting solution was exposed to radiation at a strength of 100 W for 60 minutes at 60 °C. After filtering, the precipitate was allowed to air dry. A variety of analytical methods were used to fully describe the resulting complex (a) (Fig. 1).

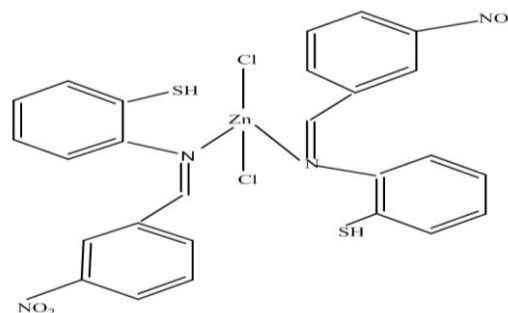


Fig.1. Structure of complex Zn-nano-complex.

2. DNA binding experiments

A new stock solution of DNA was made for each experiment, including 2 mg/ml of the material in double-distilled water with a pH adjustment to 7.2. Likewise, a stock solution containing 3×10^{-3} M of Zn-nano-complex was made using water as the solvent. An electronic absorption titration test was used to study the Zn-nano-complex and FS-DNA in order to look into DNA binding. DNA concentrations ranging from 10-130 μM was titrated with a fixed concentration of the produced metal compound (3.5×10^{-5} M) during the test. The DNA- Zn-nano-complex, solution was then allowed to equilibrate for five minutes in an incubator. After adding the DNA solution to the produced chemical, absorption spectra were recorded in the UV-Vis region and compared to the blank DNA solution. The FS-DNA solution was present or absent while measuring the fluorescence spectra. In this study, FS-DNA concentration and quantity were changed from 0-55 μM , while the concentration of the Zn-nano-complex was kept constant at 2.3×10^{-7} M. Between 330 and 410 nm, the Zn-nano-complex was released after being stimulated at 290 nm. Three distinct temperatures were used for the experiments: 303 K, 298 K, and 293 K. In order to conduct gel electrophoresis, several samples with a fixed DNA concentration of 1.4×10^{-4} M were incubated in a Tris-buffer solution for one hour with different complex concentrations ranging from 0 to 2.1×10^{-5} M. After adding loading buffer, DNA, and methylene blue to the samples, they were shaken. The resultant solution was put onto an agarose gel, and electrophoresis was run for 25 minutes at 100 V. The peaks were recorded using the UV irradiation.

2.1. Circular dichroism (CD) measurements

At a concentration of 1.4×10^{-4} mol/L DNA in a 5 mM Tris-HCl solution, CD measurements were obtained. The Zn-nano-complex concentration ratio to DNA was adjusted to (a) 0.00 and (b) 1.5×10^{-5} M. The results were collected between 210 and 380 nm in wavelength range at room temperature.

2.2 Viscosity measurements

The viscosity was measured with and without the Zn-nano-complex using an Anubelohde viscometer. The average flow durations were compared and assessed to calculate viscosity. All punctuation, grammatical, and spelling mistakes have been fixed. The data were expressed as $(\eta/\eta_0)^{1/3}$ vs. r , where r represents the concentration ratio of Zn-nano-complex to DNA. Here, η represents the viscosity of DNA with Zn-nano-complex and η_0 is the viscosity of FS-DNA alone [20].

3. RESULTS AND DISCUSSION

3.1. Characterizations of Zn-nano-complex

F-IR spectrum of Zn-nano-complex show in Fig. 2. The (C=N) stretching of the ligand is observed in the 1598 cm^{-1} and the C=C stretching absorption of the aromatic ring of this ligand are observed in a doublet at 1598 cm^{-1} . A strong absorption peak at 740 cm^{-1} is related to the stretching vibration of the C-S bond. The absorption at 618 cm^{-1} also indicates that the Zn—N [21-22].

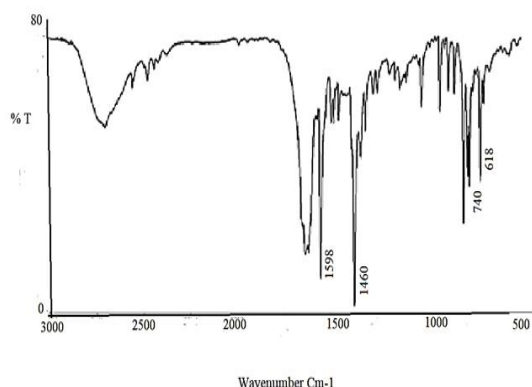


Fig. 2. FT-IR spectrum of Zn-nano-complex.

3.2 Electronic absorption spectra of Zn-nano-complex

In the electronic spectrum of (H₂L) and Zn-nano-complex show in Fig. 3. Intraligand transitions ($n \rightarrow \pi^*$) and ($\pi \rightarrow \pi^*$) are seen in the range of 290 nm to 230 nm in both compounds [23].

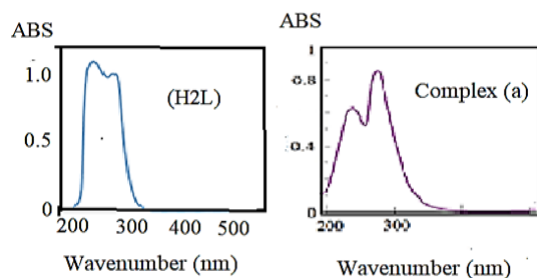


Fig. 3. Electronic absorption spectra of (H₂L) and Zn-nano-complex.

3.3. ¹H-NMR spectrum of Zn-nano-complex

NMR spectroscopy reveals that the structure of Zn-nano-complex, are held in DMSO- d₆ solution at 25°C (Fig. 4). The hydrogen atoms of the aromatic rings were seen at approximately 6–9ppm. The hydrogen atoms on the S-H and azomethine groups show two single patterns at 3.3 ppm and 2.6 ppm, respectively.

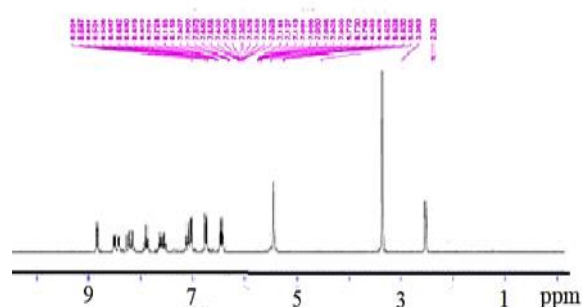


Fig. 4. ¹H- NMR spectrum of Zn-nano-complex in DMSO- d₆.

3.4 Microscopy

The SEM image of the Zn-nano-complex was shown in Fig. 5. As can be seen in the figure, the prepared sample is in the form of nanoparticles with almost uniform morphology and is porous.

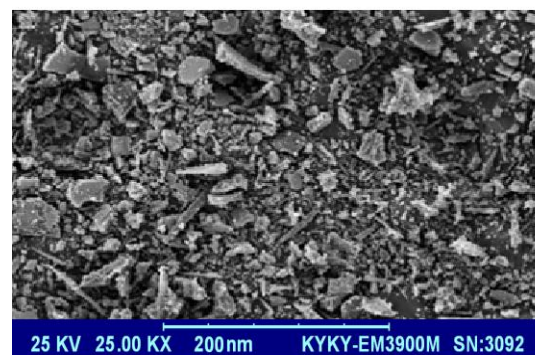


Fig. 5. SEM image of nanocrystal of Zn-nano-complex.

3.5. DNA interaction studies

3.5.1. Electronic absorption spectroscopy

Utilizing electronic absorption spectroscopy, the manner and degree of binding to DNA were determined. The synthesized Zn-nano-complex was titrated at 298 K with a constant concentration of $3.5 \times 10^{-5}\text{ M}$ in this test. The maximum absorption of the metal compound reduced when DNA was added to the produced complex solution (Fig. 6.), suggesting that the metal compound and FS-DNA interacted [24]. The binding mechanism between the Zn-nano-complex and FS-DNA is most likely groove binding, based on the observed drop in absorption intensity, or hypochromism, with minimal change in the peak locations [25].

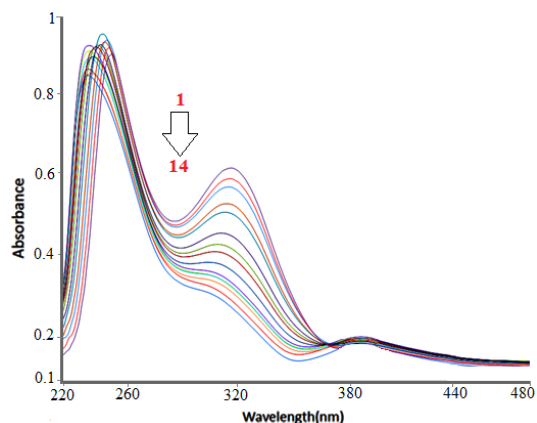


Fig. 6. UV-Vis spectra of complex (a) in the absence (line 1) and presence of diverse concentration of DNA (line 2-14) [Complex] = 3.5×10^{-5} M, [DNA] = (10-130 μ M).

The binding constant (K_b) for the interaction between the synthesized Zn(II) complex and the DNA molecule was determined using Equation (1) [27]. This equation facilitates the calculation of the binding constant, offering insights into the affinity and strength of the interaction between the complex and DNA. The method outlined by Pyle and colleagues provides a robust framework for understanding the molecular interactions at play, essential for further biochemical and biophysical analyses of the Zn-nano-complex -DNA complex. The obtained K_b value is a critical parameter, elucidating the binding efficiency and the potential biological implications of the complex in DNA-related processes.

$$\frac{[DNA]}{(\epsilon_a - \epsilon_f)} = \frac{[DNA]}{(\epsilon_b - \epsilon_f)} + 1 / K_b (\epsilon_b - \epsilon_f) \quad (1)$$

The extinction coefficient in each increment of FS-DNA solution and the Zn (II) compound (obtained from $A(\text{obs}) / [\text{Zn(II)}]$) is denoted by ϵ_a in this equation. Additionally, the extinction coefficient for the Zn-nano-complex in its completely bound form is denoted by ϵ_b , while the extinction coefficient for the free Zn-nano-complex is denoted by ϵ_f . The FS-DNA binding strength of the Zn-nano-complex was quantitatively characterized, and K_b was computed by graphing $[DNA] / (\epsilon_a - \epsilon_f)$ vs $[DNA]$ and calculating the ratio of the slope to the intercept of this plot (Fig. 7.). Zn-nano-complex has a numerical K_b value of $(5.0 \times 10^4 \pm 0.03 \text{ M}^{-1})$, which indicates the interaction between the Zn-nano-complex and DNA molecule. This value is less than the value of ethidium bromide (a traditional intercalator) that has been published ($1.4 \times 10^6 \text{ M}^{-1}$). These findings suggest that the Zn complex binding mechanism to FS-DNA differs from that of ethidium bromide (EB), as intercalation binding to DNA molecules often causes bathochromism and hypochromism of

absorption. However, we only detected hypochromism in the instance of the studied Zn compound, which is consistent with the molecular structure shown in Fig. 1 and suggests a non-interactive form of binding.

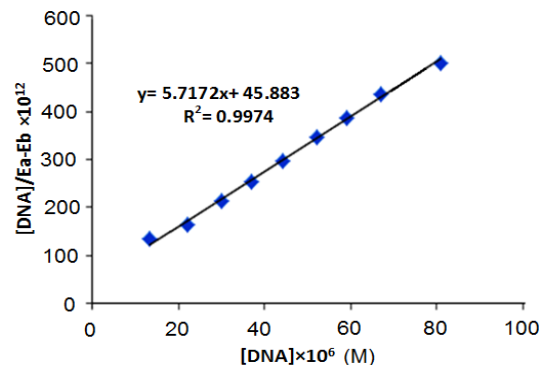


Fig. 7. Plot of $[DNA] / (\epsilon_a - \epsilon_f)$ vs $[DNA]$ in the interaction of the Zn-nano-complex with DNA molecule by electronic absorption data.

3.5.2. Fluorescence investigations

The interaction between the DNA molecule and the Zn complex was investigated further using the fluorescence technique. Investigations using electronic absorption revealed that Zn-nano-complex interactions are non-intercalative. Moreover, the Zn compound is unable to create an electrostatic connection since it is chargeless. Van der Waals forces are the sole feasible contact since the surrounding ligands of the Zn (II) ion physically prevent intercalation. Fig. 8. displays the Zn-nano-complex emission spectra with and without different concentrations of the DNA molecule. Fig. 8. displays the metal complex emission spectra with and without different concentrations of the DNA molecule. DNA quenches the Zn-nano-complex's fluorescence suggesting contact.

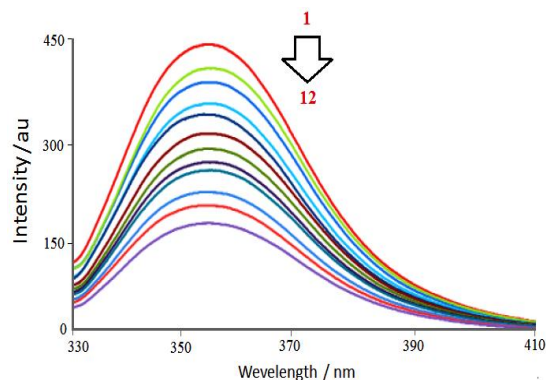


Fig 8. The emission spectra of synthesized metal complex (2.3×10^{-7} M) with different amounts of DNA, at 298 K. a) the concentration of FS-DNA grows from zero (line 1) to 55 μ M (line 12).

The method of contact was evaluated from the information that was obtained through the fluorescent light. There are basically two types of quenching mechanisms: static and dynamic. The excited fluorophore incidentally gets close to quenching chemicals during dynamic quenching. Both the viscosity and temperature of the solution have effects on the rate of quenching. With the adequate concentration of the quencher, the fluorophore and the quencher will most probably be in contact during the lifespan of the excited species. Static quenching refers to the quenching between the quencher and the fluorophore (in the ground state) to form a stable molecule. It can be differentiated between the types of quenching by their dependencies on temperature. The dynamic quenching is connected to temperature-dependent diffusion coefficients. For the verification of the quenching process, the equation of the Stern-Volmer equation was used in the analysis of the fluorescence quenching data (Equation 2).

$$F_0/F = 1 + K_{sv} [Q] = 1 + k_q \tau_0 [Q] \quad (2)$$

When quencher species (DNA) are absent, the compound's fluorescence intensity is indicated by the symbol F_0 . The symbol F stands for the compound's fluorescence intensity at different quencher concentrations. The fluorophore lifetime ($\tau_0 = 10^{-8}$ s) is represented by k_q , the Stern-Volmer quenching constant by K_{sv} , and the quencher concentration by $[Q]$ [28].

Plotting F_0/F versus $[DNA]$ allowed for the determination of the Stern-Volmer quenching constant (K_{sv}) (Fig. 9). Using K_{sv}/τ_0 , the value of k_q was calculated at three distinct temperatures: 293 K, 298 K, and 303 K. As the temperature rises, both k_q and K_{sv} drop, as shown by the data in Table 1. Notably, the static quenching process is indicated by the value of k_q above $2.0 \times 10^{10} M^{-1}s^{-1}$ [29].

The fluorescence test can be used to calculate the titration information, which can then be used to obtain binding constant (K_b) values and binding sites (n) using Equation 3 [30].

$$\log((F_0 - F)/F) = \log K_b + n \log [Q] \quad (3)$$

Where the definitions of F_0 , F , and $[Q]$ are identical to those found in Equation (2). Equation (3) (Fig.

10) was utilized to determine the parameters n and K_b , respectively, by calculating the intercept and slope of $\log((F_0 - F)/F)$ against $\log([DNA]/\mu M)$. The reduction in K_b with increasing temperature [31] suggests that the interaction between DNA and the chemical (a) is probably exothermic, according to the findings shown in Table 1. Consequently, the Zn (II) complex has a single distinct set of binding sites on DNA [32]. There are nearly as many binding sites (n) as there are. The results of these research demonstrate that the value of K_b ascertained by UV-Vis and fluorescence studies is same.

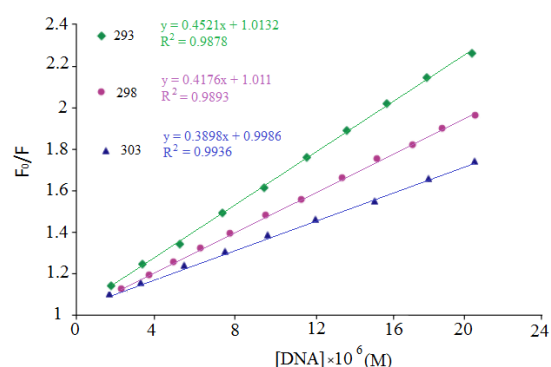


Fig. 9. The a) synthesized metal complex Stern-Volmer graphs at three different temperatures (303, 298 and 293 K).

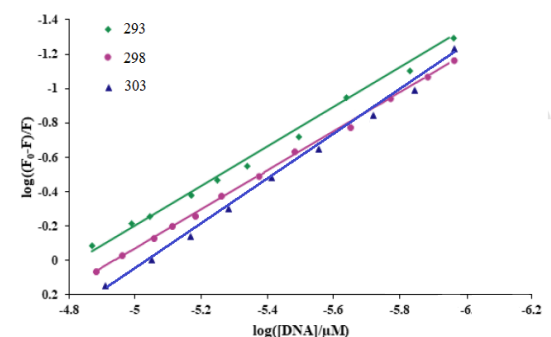


Fig. 10. $\log ((F_0 - F)/F)$ versus. $\log ([DNA]/\mu M)$ for the fluorescence titration of the synthesized metal complex with DNA at diverse temperatures (303, 298 and 293 K)

Table 1. The values of K_{sv} , k_q , n and thermodynamic factors for the interaction of a) the Zn-nano-complex with DNA calculated from the fluorescence studies at different temperatures of (303, 298 and 293 K).

Complex	T (K)	$K_{sv} \times 10^5 (M^{-1})$	$k_q \times 10^{13} (M^{-1}s^{-1})$	n	$K_b \times 10^4 (M^{-1})$		$\Delta G^\circ (kJ/mol)$	$\Delta H^\circ (kJ/mol)$	$\Delta S^\circ (J/mol.K)$
					Fluorescence	UV-Vis			
Zn-nano-complex	303	3.89±0.01	3.89±0.01	0.99	1.6 ± 0.02	5.0± 0.03	-40.84±0.02	-6.6	0.013
	298	4.17±0.01	4.17±0.01	1.01	1.9 ± 0.01	4.0± 0.03	-38.94±0.04	2.3	0.016
	293	4.52±0.02	4.52±0.02	1.01	2.2 ± 0.04	5.0± 0.03	-39.02±0.01	-7.3	0.013

3.5.3. Data on fluorescence and thermodynamic parameter computation

The thermodynamics of the reaction between the aforementioned substances and FS-DNA must be understood in order to distinguish between standard entropy (ΔS°), enthalpy (ΔH°), and Gibbs free energy (ΔG°) changes. Thermodynamic factors may be used to predict the binding interactions (hydrophobic, hydrogen bonding, van der Waals, and electrostatic) that take place between FS-DNA and small molecules. Using the given K_b values at various temperatures and the van't Hoff equation (4), we were able to determine both ΔS° and ΔH° [33].

$$\ln K_b = -\Delta H^\circ/RT + \Delta S^\circ/R \quad (4)$$

The values of ΔS° and ΔH° were obtained by plotting $\ln K_b$ vs $1/T$ (Fig. 11.). The slope ($-\Delta H^\circ/R$) represents ΔH° and the intercept ($\Delta S^\circ/R$) represents ΔS° . Table 1. shows the ΔG° values calculated using equation (5) for the interaction between the Zn (II) compound and DNA.

$$\Delta G^\circ = \Delta H^\circ - T\Delta S^\circ = -RT \ln K_b \quad (5)$$

Electrostatic interactions have small or no enthalpy change and positive entropy change. Hydrogen bonding and van der Waals interactions have negative values of ΔS° and ΔH° , while hydrophobic interactions have positive values of ΔS° and ΔH° . Table 1. shows negative ΔH° and ΔS° , indicating Zn (II) complex binds DNA grooves via H-bonding and van der Waals forces. Negative values of ΔG° indicate that the reactions occur spontaneously. Upon increasing temperature, the K_b values decrease, which is consistent with the exothermic interaction of Zn-nano-complex with DNA as indicated by the negative values of ΔH° [34]. (Table 1).

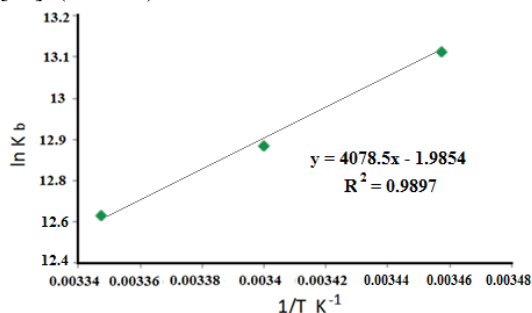


Fig. 11. The van't Hoff plot in the interaction of Zn-nano-complex with FS-DNA at diverse temperatures (303, 298 and 293 K).

3.5.4. Viscosity measurement

In the absence of crystallographic data, viscometric testing provides a practical method for detecting changes in DNA shape. For intercalative binding, the target ligand increases the length and viscosity of the DNA by separating FS-DNA base pairs [35, 36]. Electrostatic or groove binding are examples of non-intercalative binding that have no

effect on DNA viscosity. FS-DNA's viscosity was assessed both with and without the generated complex. With t representing the time of the sample solution and t_0 representing the time of the blank solution, the formula that was used was $\eta = (t - t_0)/t_0$. Fig. 12 shows that the relative viscosity of FS-DNA remained constant while the quantity of complex increased when Zn complex coexisted in the FS-DNA solution. These results demonstrate that there is no intercalation in the binding process.

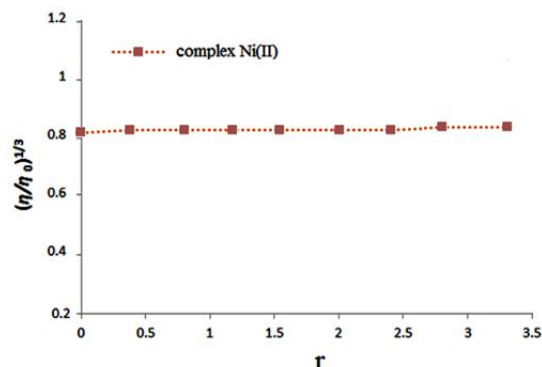


Fig. 12. The results of increasing amounts of Zn-nano-complex on the relative viscosity of FS-DNA at 298 K. The concentration of FS-DNA was 1.4×10^{-4} mol L⁻¹.

3.5.5. CD analysis

DNA and other optically active substances are commonly analyzed for structure using the circular dichroism (CD) spectral method. This spectrum is a powerful tool for examining a compound's chiral characteristics. It also detects changes in the secondary structure of proteins and DNA as they interact with complexes and medications, providing important information about how they bind. It has been demonstrated that CD spectroscopy may successfully identify minute conformational changes in DNA structure that occur during binding. The mechanism of interaction between complexes and DNA affects the sensitivity of CD signals. Because DNA is right-handed helical, FS-DNA solutions show a negative band at 230 nm and a positive band at 275 nm because to base stacking. The sensitivity of these bands is strongly affected by the mechanism of interaction with chemicals. Modifications in DNA structure may be indicated by changes in CD signals. In the right-handed B conformation of FS-DNA, intercalation processes strengthen base stacking interactions, stabilizing DNA conformations and raising the intensities of both bands. On the other hand, base stacking and helicity bands are only slightly disturbed by tiny molecules that attach non-intercalatively, such as via groove and electrostatic binding. Fig. 13 displays the circular dichroism spectrum of DNA with and without Zn-nano-complex. The findings

demonstrate that base stacking is decreased and structural changes in DNA are induced by contacting the target complex. Our theory of a groove binding mode is supported by these CD spectrum alterations, which point to a non-intercalative manner of binding.

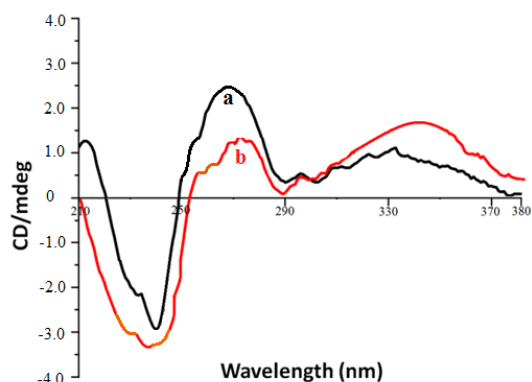


Fig. 13. The circular dichroism spectrum of DNA in the absence and presence of complex (a). The concentration of DNA was 1.4×10^{-4} mol L⁻¹. The concentration ratio of Zn compound to [DNA] was (a) 0.00, (b) 1.5×10^{-5} mol L⁻¹.

3.5.6. Gel retardation experiment

The technique of gel electrophoresis test is employed to investigate DNA movement through a gel matrix in the presence of an electric field [37]. We used this experiment to demonstrate compound-DNA interaction by observing variations in DNA electrophoretic migration in the presence of varying amounts of produced Zn-nano-complex. (Figure 14). The weight, size, and shape of DNA sites are increased when Zn-nano-complex binds to them, which slows electrophoretic mobility. The electropherogram demonstrates interactions by demonstrating that Zn (II) in DNA samples (lanes 2–8) prevents DNA movement. Findings from the complex and DNA were consistent.

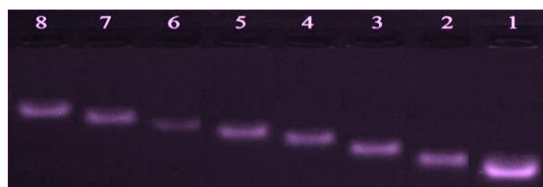


Fig. 14. Gel electrophoresis of FS-DNA in the absence and presence of different amounts of Zn (II) complex at 25 °C. Lane 1: DNA control; Lane 2–8: DNA + Zn (II) complex (0.3, 0.6, 0.9, 1.2, 1.5, 1.8, 2.1 $\times 10^{-5}$ M, respectively).

4. CONCLUSIONS

In this study a nano-complex with the formula $[\text{Zn}(\text{HL})_2\text{Cl}_2]$ was synthesized using sonochemical method. Zn-nano-complex was identified by FT-IR, UV-Vis, ¹H-NMR and Emission Scanning

Electron Microscope (SEM). Structural studies showed the Schiff base ligand coordinating to the metal ion in a 1:2 molar ratio through nitrogen atoms. The geometry of Zn-nano-complex is tetrahedral. UV-Vis analysis showed that Zn complex binds to DNA with a favorable binding constant. The fluorescence investigation data showed that a DNA molecule quenched the Zn-nano-complex. The quenching occurred through a static mechanism, and the K_b values decreased as the temperature increased, indicating an exothermic interaction. Fluorescence data yielded thermodynamic parameters showing the metal complex is held in DNA grooves by van der Waals forces and hydrogen bonding.

Acknowledgments

The authors thank the University of Sistan and Baluchestan, Zahedan, Iran for the support of this research work.

REFERENCES

- [1] L. H. Abdel-Rahman, R. M. El-Khatib, L. A. E. Nassr, and A. M. Abu-Dief, DNA Binding Ability Mode, Spectroscopic Studies, Hydrophobicity, and in Vitro Antibacterial Evaluation of Some New Fe(II) Complexes Bearing ONO Donor Amino Acid Schiff Bases, *Arab. J. Chem.* 10 (2017) S1834-S1846.
- [2] H. Kargar, M. Fallah-Mehrjardi, R. Behjatmanesh-Ardakani, Kh. Sh. Munawar, M. Bahadorie, and M. Moghadam, Synthesis, spectral characterization, and theoretical investigation of Pd(II) complex incorporating unsymmetrical tetradentate Schiff base ligand and its application in Suzuki–Miyaura cross-coupling reaction, *Inorg. Chem. Res.* 6 (2022) 76-83.
- [3] M. Asadollahi, H. Golchoubian, and A. Shirvan, Mononuclear Nickel(II) and Zinc(II) Complexes with N-(2-propanamide)-2-picolyamine Ligand: Synthesis, Chromotropism Properties and DFT Calculations, *Inorg. Chem. Res.* 6 (2022) 146-154.
- [4] M. Rezaeivala, Synthesis, Characterization and Theoretical Studies of a New Macroacyclic SchiffBase Ligand Containing Piperazine Moiety and Related Mn(II), Cu(II), Ni(II) and Cd(II) Complexes, *Inorg. Chem. Res.* 1 (2017) 85-92.
- [5] R. Golbedaghi, A. Mohammadzaheri, M. Liyaghati-Delshad, N. Ajami, and M. Mahdavi Lasibi, Cu(II) Complexes of a Tripodal Tetraamine Incorporating a Pendant Arm and Related Schiff Base Ligand; X-ray Crystal Structure and Spectral Studies *Inorg. Chem. Res.* 7 (2023) 22-26.

- [6]A. Sahraei, H. Kargar, M. Hakimi and M. N. Tahir, Distorted square-antiprism geometry of new zirconium (IV) Schiff base complexes: Synthesis, spectral characterization, crystal structure and investigation of biological properties, *J. Mol. Struct.* 1149 (2017) 576-584.
- [7]A. Zamanpour, M. Asadi and G. Absalan, New Tetraaza Schiff Base Ligands and Their Complexes: Synthesis, Characterization and Thermodynamic Studies, *Inorg. Chem. Res.* 1 (2016) 59-68.
- [8]H. Kargar, M. Fallah-Mehrjardi, R. Behjatmanesh-Ardakani and Kh. Sh. Munawar, New Copper (II) Complexes with Benzimidazole and Benzoxazole Heterocyclic Ligands: Synthesis, Spectral Characterization, FMO, MEP, NBO, and DFT Study, *Inorg. Chem. Res.* 6 (2022) 48-57.
- [9]J. Joseph, K. Nagashri, and G. Ayisha Bibin Rani, Synthesis, characterization an antimicrobial activities of copper complexes derived from 4-aminoantipyrine derivatives Source Information, *J. Saudi Chem. Soc.* 17 (2013) 285-294.
- [10]Ö. Güngör, M. Çeşme, M. Emin Çınar, and A. Gölcü, The new metal-based compound from anticancer drug cytarabine: Spectral, electrochemical, DNA-binding, antiproliferative effect and in silico studies, *J. Mol. Struct.* 118 (2019) 532-543.
- [11]R. G. Mohamed, F. M. Elantabli, A. A. Abdel aziz, H. Moustafa, and S. M. El-Medani, *J. Mol. Struct.* 1176 (2019) 501-514.
- [12]B. Shafaatian, S. S. Mousavi, and S. Afshari, Synthesis, characterization, spectroscopic and theoretical studies of new zinc(II), copper(II) and nickel(II) complexes based on imine ligand containing 2-aminothiophenol moiety, *J. Mol. Struct.* 1123 (2016) 191-198.
- [13]G. Y. Nagesh, and B. H. M. Mruthyunjayaswamy, Synthesis, characterization and biological relevance of some metal (II) complexes with oxygen, nitrogen and oxygen (ONO) donor Schiff base ligand derived from thiazole and 2-hydroxy-1-naphthaldehyde, *J. Mol. Struct.* 1085 (2015) 198-206.
- [14]Z. Abbasi, M. Salehi, A. Khaleghian, and M. Kubicki, In vitro cytotoxic activity of a novel Schiff base ligand derived from 2-hydroxy-1-naphthaldehyde and its mononuclear metal complexes, *J. Mol. Struct.* 1173 (2018) 213-220.
- [15]A. Izadyar, and H. Mansouri-Torshizi, E. Dehghanian, S. Shahraki, Spectroscopy, docking and molecular dynamics studies on the interaction between *cis* and *trans* palladium-alanine complexes with calf-thymus DNA and antitumor activities, *J. Coord. Chem.* 76 (3-4) (2023) 519-542.
- [16]T. Kondori, N. Akbarzadeh-T, and C. Graiff, Synthesis, X-ray structural analysis, antibacterial and DNA-binding studies of a lanthanum bis-(5, 5'-dimethyl-2, 2'-bipyridine) complex, *J. Iran. Chem. Soc.* 16(9) (2019) 1827-1838.
- [17]S. Mudasir, K. Wijaya, E. T. Wahyuni, N. Yoshioka, and H. Inoue, Salt-dependent binding of iron(II) mixed-ligand complexes containing 1,10-phenanthroline and dipyrido[3,2-a:2',3'-c]phenazine to calf thymus DNA, *Biophys. Chem.* 121(1) (2006) 44-50.
- [18]P. Gurumoorthy, D. Mahendiran, D. Prabhu, C. Arulvasu, and A. K. Rahman, Mixed-ligand copper (II) phenolate complexes: Synthesis, spectral characterization, phosphate-hydrolysis, antioxidant, DNA interaction and cytotoxic studies, *J. Mol. Struct.* 1080 (2015) 88-98
- [19]M. Fazli, N. Akbarzadeh-T, H. Beitollahi, M. Dus'ek, and V. Eigner, New Schiff base ligand N-(2-hydroxy-1-naphthylidene)- 2-methyl aniline and its nano-sized copper(II) complex: synthesis, characterization, crystal structure and application as an electrochemical sensor of 2- phenylphenol in the presence of 4-chlorophenol, *J. Mater. Sci.: Mater. Electron.*, 32 (2021) 25118-25136.
- [20]G. Cohen, and H. Eisenberg, Viscosity and sedimentation study of sonicated DNA-proflavine complexes. *Biopolymers*, 8(1) (1969) 45-55.
- [21]H. Kargar, V. Torabi, A. Akbari, R. Behjatmanesh-Ardakani, and M. N. Tah, Synthesis, characterization, crystal structure and DFT studies of a palladium (II) complex with an asymmetric Schiff base ligand, *J. Mol. Struct.* 1179 (2019) 732-738.
- [22]Kargar, and R. Kia, Synthesis and Crystal Structures of Three New Hetero-binuclear Hg(II)-Cu(II) Schiff Base Complexes, *Inorg. Chem. Res.* 1 (2017) 40-49.
- [23]R. Alizadeh, and V. Amani, Syntheses, crystal structures, and photoluminescence of three cadmium(II) coordination complexes based on bipyridine ligands with different positioned methyl substituents, *J. Inorg. Chim. Acta.* 443 (2016)151-159.
- [24]S. Kashanian, M. M. Khodaei, and P. Pakravan, Spectroscopic studies on the interaction of isatin with calf thymus DNA, *DNA and Cell Biology.* 29(10) (2010) 639-648.
- [25]K. Abdi, H. Hadadzadeh, M. Salimi, J. Simpson, and A. D. Khalaji, A mononuclear

- copper(II) complex based on the polypyridyl ligand 2,4,6-tris(2-pyridyl)-1,3,5-triazine (tptz), [Cu(tptz)₂]²⁺: X-ray crystal structure, DNA binding and *in vitro* cell cytotoxicity. *Polyhedron*.44 (1) (2012)101-112.
- [26]J. R. Lakowicz, and G. Weber, Quenching of protein fluorescence by oxygen. Detection of structural fluctuations in proteins on the nanosecond time scale, *J. Biochem.* 12(21) (1973) 4171-4179.
- [27]M. Kumari, J. K. Maurya, U. K. Singh, A. B. Khan, M. Ali, P. Singh, and R. Patel, Spectroscopic and docking studies on the interaction between pyrrolidinium based ionic liquid and bovine serum albumin, *Spectrochim. Acta. A Mol. Biomol. Spectrosc.* 124 (2014) 349-356.
- [28]A. Belatik , S. Hotchandani, J. Bariyanga, and H. A. Tajmir-Riahi, Binding sites of retinol and retinoic acid with serum albumins, *Eur. J. Med. Chem.* 48 (2021) 114-123.
- [29]H. Mansouri-Torshizi, S. Zareian-Jahromi, Kh. Abdi, and M. Saeidifar, Nonionic but water soluble,[Glycine-Pd-Alanine] and [Glycine-Pd-Valine] complexes. Their synthesis, characterization, antitumor activities and rich DNA/HSA interaction studies, *J. Biomol. Struct. Dyn.* 37(13) (2019) 3566-3582.
- [30] M. Saeidifar, H. Mansouri-Torshizi, Y. Palizdar, M. Eslami-Moghaddam, A. Divsalar, and A. A. Saboury, Synthesis, characterization, cytotoxicity and DNA binding studies of a novel anionic organopalladium (II) complex, *Acta. Chimica. Slovenica.* 61(1) (2014) 126–136.
- [31]A. Heydari, and H. Mansouri-Torshizi, Synthesis, characterization, cytotoxicity and DNA binding studies of a novel anionic organopalladium (II) complex, *RSC Advances.* 6(98) (2016) 96121-96137.
- [32]H. Mahaki, H. Tanzadehpanah, O. K. Abou-Zied, N. H. Moghadam, A. Bahmani, S. Salehzadeh, D. Dastan, and M. Saidijam, Cytotoxicity and antioxidant activity of Kamolonol acetate from *Ferula pseudalliacea*, and studying its interactions with calf thymus DNA (ct-DNA) and human serum albumin (HSA) by spectroscopic and molecular docking techniques, *Process Biochem.* 79 (2019) 203-213.
- [33]L. S. Lerman, Structural considerations in the interaction of DNA and acridines, *J. Mol. Biol.* 3(1) (1961) 18-IN14.
- [34]Z. Moradi, M. Khorasani-Motlagh, A. R. Rezvani, and M. Noroozifar, Evaluation of DNA, BSA binding, and antimicrobial activity of new synthesized neodymium complex containing. 2-dimethyl 1-10-phenanthroline. *J. Biomol. Struct. Dyn.*36 (3) (2018) 779-794.
- [35]]T. Kondori, O. Shahraki, N. Akbarzadeh-T, and Z. Aramesh-Boroujeni, Two Novel Bipyridine-based Cobalt (II) Complexes: Synthesis, Characterization, Molecular Docking, DNA-Binding and Biological Evaluation, *J. Biomol. Struct. Dyn.* 39(2) (2020) 1-27.
- [36]E. Grueso, G. Lopez-Perez, M. Castellano, and R. Prado-Gotor, Thermodynamic and structural study of phenanthroline derivative ruthenium complex/DNA interactions: probing partial intercalation and binding properties, *J. Inorg. Biochem.* 106(1) (2012) 1-9.
- [37]S. Zareian-Jahromi, and H. Mansouri-Torshizi, Synthesis, characterization, DNA and HSA binding studies of isomeric Pd (II) antitumor complexes using spectrophotometry techniques, *J. Biomol. Struct. Dyn.* 36(5) (2018) 1329-1350.



COPYRIGHTS

© 2022 by the authors. Licensee PNU, Tehran, Iran. This article is an open access article distributed under the terms and conditions of the Creative Commons Attribution 4.0 International (CC BY4.0) (<http://creativecommons.org/licenses/by/4.0>)

مطالعات فلورسانس و بررسی طیف‌سنجی جذب الکترونیکی برهم‌کنش بین نانو کمپلکس شیف باز روی (II) با FS-DNA

ندا بارکزایی، نیلوفر اکبرزاده تربتی*

گروه شیمی، دانشگاه سیستان و بلوچستان، زاهدان، ایران

* E-mail: n.akbarzadeh@chem.usb.ac.ir

تاریخ دریافت: ۱ مرداد ۱۴۰۳ تاریخ پذیرش: ۱ شهریور ۱۴۰۳

چکیده

در این پروژه در قسمت اول لیگاند پایه شیف (3-nitrobenzaldehyde + 2-aminothiophenol = H₂L) تهیه شد. سپس یک نانو کمپلکس با فرمول (a) [Zn(HL)₂Cl₂] با استفاده از روش سونوشیمیایی سنتز شد. (a) [Zn(HL)₂Cl₂] توسط UV-Vis، FT-IR، ¹H-NMR و میکروسکوپ الکترونی روبشی (SEM) شناسایی شد. نتایج طیف‌سنجی نشان داد که لیگاند H₂L از طریق اتم N به فلز کوردینه شده است. طیف FT-IR ترکیب (a) باند ارتعاشی گروه ایمین (C = N) را در ۱۶۸۰-۱۶۰۰ cm⁻¹ نشان داد. مطالعات به دست آمده از طیف‌سنجی UV-Vis انتقالات درون لیگاند $\pi \rightarrow \pi^*$ و $n \rightarrow \pi^*$ را تایید می‌کند. FS-DNA (اسپرم ماهی قزل‌آلا) و کمپلکس (a) با استفاده از طیف‌سنجی UV-Vis، طیف‌سنجی فلورسانس و الکتروفورز ژل مورد بررسی قرار گرفتند. از معادله استرن-ولمر برای محاسبه ثابت اتصال (K_b) و ثابت خاموش شدن دو مولکولی ظاهری (k_q) برای FS-DNA استفاده شد. بر اساس تجزیه و تحلیل پارامترهای ترمودینامیکی (ΔG° و ΔS° ، ΔH°) نیروهای واندروالس و پیوندهای هیدروژنی در برهم‌کنش بین DNA و کمپلکس روی (II) مهم هستند. مکانیسم برهم‌کنش به حالت اتصال شیباری تعیین شد. این نتایج تأثیرات پیچیده این مجموعه را بر ساختار DNA و نیاز به استفاده از انواع تکنیک‌های تحلیلی به منظور بررسی کامل برهم‌کنش‌های فلز-DNA را برجسته می‌کند.

کلید واژه‌ها

شیف باز؛ DNA اسپرم ماهی؛ برهم‌کنش واندروالس؛ الکتروفورز ژل.